

Pion Interferometry for a Granular Source of Quark-Gluon Plasma Droplets

W. N. Zhang^{1,2}, M. J. Efaaf¹, and Cheuk-Yin Wong^{2,3}

¹*Department of Physics, Harbin Institute of Technology, Harbin, 150006, P. R. China*

²*Physics Division, Oak Ridge National Laboratory, Oak Ridge, TN 37831, U.S.A.*

³*Department of Physics, University of Tennessee, Knoxville, TN 37996, U.S.A.*

(Dated: July 8, 2018)

We examine the two-pion interferometry for a granular source of quark-gluon plasma droplets. The evolution of the droplets is described by relativistic hydrodynamics with an equation of state suggested by lattice gauge results. Pions are assumed to be emitted thermally from the droplets at the freeze-out configuration characterized by a freeze-out temperature T_f . We find that the HBT radius R_{out} decreases if the initial size of the droplets decreases. On the other hand, R_{side} depends on the droplet spatial distribution and is relatively independent of the droplet size. It increases with an increase in the width of the spatial distribution and the collective-expansion velocity of the droplets. As a result, the value of R_{out} can lie close to R_{side} for a granular quark-gluon plasma source. The granular model of the emitting source may provide an explanation to the RHIC HBT puzzle and may lead to a new insight into the dynamics of the quark-gluon plasma phase transition.

PACS numbers: 25.75.-q, 25.75.Nq, 25.75.Gz

Recent experimental pion HBT measurements at RHIC give the ratio of $R_{\text{out}}/R_{\text{side}} \approx 1$ [1, 2] which is contrary to many theoretical expectations [1, 3, 4, 5, 6, 7, 8]. This RHIC HBT puzzle hints that the pion emitting time may be very short [9, 10]. Various models have been put forth to explain the HBT puzzle [11, 12, 13, 14, 15, 16].

In this paper, we propose a simple model of a granular source of quark-gluon plasma droplets [17, 18, 19, 20, 21] to explain the puzzle. The possible occurrence of a granular structure of droplets during a first-order QCD phase transition was discussed by Witten [22] and examined by many authors [23, 24, 25, 26, 27]. We assume that pions are emitted thermally from hydrodynamically expanding droplets at a freeze-out temperature T_f and use relativistic hydrodynamics to describe the evolution of quark-gluon plasma droplets with an equation of state suggested by QCD lattice gauge results [3, 28, 29, 30]. The two-pion correlation function can then be calculated after knowing the hydrodynamical solution [20, 21, 31]. As the average freeze-out time is approximately proportional to the initial droplet size, we would like to see whether a granular source with many smaller droplets and their corresponding smaller freeze-out times will lead to R_{out} close to R_{side} .

We study a quark-gluon plasma with no net-baryon content and use a equation of state of the fluid in terms of the entropy density function $s(T)$ by [3, 28, 29, 30]

$$\frac{s(T)}{s_c} = \left[\frac{T}{T_c} \right]^3 \left(1 + \frac{d_Q - d_H}{d_Q + d_H} \tanh \left[\frac{T - T_c}{\Delta T} \right] \right). \quad (1)$$

Here d_Q and d_H are respectively the degrees of freedom in the quark-gluon plasma phase and the hadronic phase, $T_c \approx 160$ MeV is the transition temperature, s_c is the entropy density at T_c , and ΔT (between 0 and $0.1T_c$) is the width of the transition [3, 28]. In this paper, we take $d_Q = 37$, $d_H = 3$, $T_c = 160$ MeV as in Ref. [3, 28], and take $\Delta T = 0.05T_c$.

We shall make the approximation that the hydrodynamical solution for many independent droplets can be obtained by superposing the hydrodynamical solution of a single droplet. It suffices to focus attention on the hydrodynamics of a single droplet. Knowing the entropy density $s(T)$, one can get the pressure p , energy density ϵ , and the velocity of sound c_S in the droplet with the following equations as in Ref. [3, 28],

$$p = \int_0^T dT' s(T'), \quad \epsilon = Ts - p, \quad c_S^2 = \frac{dp}{d\epsilon}. \quad (2)$$

The energy momentum tensor of a thermalized fluid cell in the center-of-mass frame of the droplet is [3, 32, 33]

$$T^{\mu\nu}(x) = [\epsilon(x) + p(x)] u^\mu(x) u^\nu(x) - p(x) g^{\mu\nu}, \quad (3)$$

where x is the space-time coordinate, $u^\mu = \gamma(1, \mathbf{v})$ is the 4-velocity of the cell, and $g^{\mu\nu}$ is the metric tensor. With the local conservation of energy and momentum, one can follow Rischke and Gyulassy and get the equations for spherical geometry as [3, 28]

$$\partial_t E + \partial_r [(E + p)v] = -F, \quad (4)$$

$$\partial_t M + \partial_r (Mv + p) = -G, \quad (5)$$

where $E \equiv T^{00}$, $M \equiv T^{0r}$,

$$F = \frac{2v}{r}(E + p), \quad G = \frac{2v}{r}M. \quad (6)$$

We assume the initial conditions as [3, 28]

$$\epsilon(0, r) = \begin{cases} \epsilon_0, & r < r_d, \\ 0, & r > r_d, \end{cases} \quad v(0, r) = \begin{cases} 0, & r < r_d, \\ 1, & r > r_d, \end{cases} \quad (7)$$

where $\epsilon_0 = 1.875T_c s_c$ [3, 28] is the initial energy density of the droplets, and r_d is the initial droplet radius. Using the Harten-Lax-van Leer-Einfeldt (HLLE) scheme

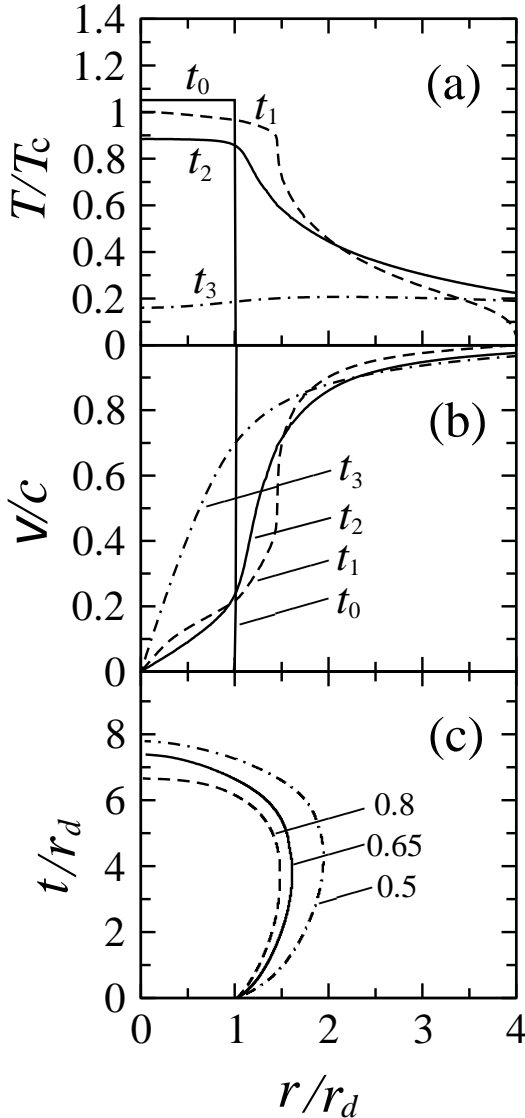


FIG. 1: (a) Temperature profile and (b) velocity profile for the droplet at $t_n = 3n\lambda r_d$, $\lambda = 0.99$. (c) Isotherms for the droplet.

[3, 28, 34, 35] and the relation of $p = p(\epsilon)$ obtained from Eqs. (1) and (2), one can get the solution of the hydrodynamical equations for $F = G = 0$. One then obtains the solution for Eqs. (4) and (5) by using the Sod’s operator splitting method [3, 28, 36]. The grid spacing for the HLLE scheme is taken to be $\Delta x = 0.01r_d$, and the time step for the HLLE scheme and Sod’s method corrector is $\Delta t = 0.99\Delta x$ [3, 28]. Figure 1(a) and 1(b) show the temperature and velocity profiles of the droplet. Figure 1(c) gives the isotherms for the droplet.

The two-particle Bose-Einstein correlation function is defined as the ratio of the two-particle momentum distribution $P(k_1, k_2)$ to the product of the single-particle momentum distribution $P(k_1)P(k_2)$. For a chaotic pion-emitting source, $P(k_i)$ ($i = 1, 2$) and $P(k_1, k_2)$ can be

expressed as [37]

$$P(k_i) = \sum_{X_i} A^2(k_i, X_i), \quad (8)$$

$$P(k_1, k_2) = \sum_{X_1, X_2} \left| \Phi(k_1, k_2; X_1, X_2) \right|^2, \quad (9)$$

where $A(k_i, X_i)$ is the magnitude of the amplitude for emitting a pion with 4-momentum $k_i = (\mathbf{k}_i, E_i)$ in the laboratory frame at X_i and is given by the Bose-Einstein distribution in the local rest frame of the source point. $\Phi(k_1, k_2; X_1, X_2)$ is the two-pion wave function. Neglecting the absorption of the emitted pions by other droplets, $\Phi(k_1, k_2; X_1, X_2)$ is simply

$$\begin{aligned} \Phi(k_1, k_2; X_1, X_2) &= \frac{1}{\sqrt{2}} \left[A(k_1, X_1)A(k_2, X_2)e^{ik_1 \cdot X_1 + ik_2 \cdot X_2} \right. \\ &\quad \left. + A(k_1, X_2)A(k_2, X_1)e^{ik_1 \cdot X_2 + ik_2 \cdot X_1} \right]. \end{aligned} \quad (10)$$

Using the components of “out” and “side” [5, 7, 38, 39] of the relative momentum of the two pions, $q = |\mathbf{k}_1 - \mathbf{k}_2|$, as variables, we can construct the correlation function $C(q_{\text{out}}, q_{\text{side}})$ from $P(k_1, k_2)$ and $P(k_1)P(k_2)$ by summing over \mathbf{k}_1 and \mathbf{k}_2 for each $(q_{\text{out}}, q_{\text{side}})$ bin. The HBT radius R_{out} and R_{side} can then be extracted by fitting the calculated correlation function $C(q_{\text{out}}, q_{\text{side}})$ with the following parametrized correlation function

$$C(q_{\text{out}}, q_{\text{side}}) = 1 + \lambda e^{-q_{\text{out}}^2 R_{\text{out}}^2 - q_{\text{side}}^2 R_{\text{side}}^2}. \quad (11)$$

The explicit procedure for calculating the two-pion correlation function is as follows.

Step 1: select the emission points of the two pions randomly on the space-time freeze-out surfaces of the droplets, and get their space-time coordinate X_1 and X_2 in the laboratory frame.

Step 2: generate the momenta k'_1 and k'_2 of the two pions in local frame according the Bose-Einstein distribution characterized by the temperature T_f , and obtain their momenta k_1 and k_2 in the laboratory frame by Lorentz transforms.

Step 3: calculate $[E'_1/E_1][E'_2/E_2]$ for $P(k_1)P(k_2)$ and $[E'_1/E_1][E'_2/E_2] \cos[(k_1 - k_2)(X_1 - X_2)]$ for $P(k_1, k_2)$, and accumulate them in the corresponding $(q_{\text{out}}, q_{\text{side}})$ bin.

Step 4: repeat steps 1 through 4 many times to get the correlation function within a certain accuracy.

We first examine the two-pion correlation function for a singlet droplet source. By fitting the two-dimension correlation function $C(q_{\text{out}}, q_{\text{side}})$ obtained with the above steps with Eq. (11), we get the parameters R_{out} , R_{side} , and λ simultaneously. In our calculations, the average transverse momenta of the pions are integrated over. The average transverse momenta of the pions in our fitting samples are 307, 329, and 386 MeV for $T_f = 0.8T_c$, $0.65T_c$, and $0.5T_c$, respectively. The reason for a larger average

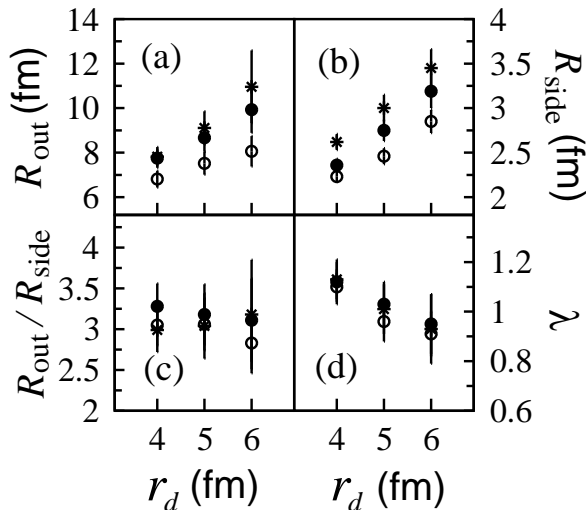


FIG. 2: The two-pion interferometry results for the one-droplet source as a function of the initial droplet radius r_d . The symbols \circ , \bullet , and \star are for the freeze-out temperatures $T_f = 0.80T_c$, $T_f = 0.65T_c$, and $T_f = 0.50T_c$, respectively.

transverse momentum to associate with a smaller freeze-out temperature is due to the larger average expansion velocity in the case of a smaller freeze-out temperature. Figure 2(a), 2(b), 2(c), and 2(d) show the HBT results R_{out} , R_{side} , $R_{\text{out}}/R_{\text{side}}$, and λ as a function of the initial radius r_d of the droplet, for the freeze-out temperatures $T_f = 0.80T_c$ (symbol \circ), $T_f = 0.65T_c$ (symbol \bullet), and $T_f = 0.50T_c$ (symbol \star). It can be seen that the HBT radii R_{out} and R_{side} increase linearly with r_d , but the ratio $R_{\text{out}}/R_{\text{side}}$ is about 3 within the errors. The radius R_{side} reflects the spatial size of the source and the radius R_{out} is related to the lifetime of the source [5, 7, 38, 39]. From the hydrodynamical solution in figure 1(c), both the average freeze-out time and freeze-out radial distance increase with r_d for different T_f . As a consequence, $R_{\text{out}}/R_{\text{side}}$ is insensitive to the values r_d and T_f . The value of $R_{\text{out}}/R_{\text{side}} \sim 3$ for a single droplet is however much larger than the observed values [1, 2]. In our calculations, we did not including resonances in the hadronic phase. If we take the hypothetical case of $d_Q/d_H = 3$ to include a resonance gas in the hadronic phase, as discussed by Rischke and Gyulassy [3], we find that the ratio of $R_{\text{out}}/R_{\text{side}}$ is about 2.75. It is still much larger than the observed values [1, 2]. In Fig. 1 (d), the values of λ for $r_d = 4$ fm are larger than unity. This is a non-Gaussian correlation function effect, and the effect is larger for a wider correlation function, corresponding to a smaller source.

As the average freeze-out time is proportional to the initial radius of the droplet, the freeze-out time and R_{out} decreases if the initial radius of the droplet decreases. On the other hand, R_{side} increases if the width of the droplet spatial distribution increases. A variation of the droplet size and the width of droplet spatial distribution can result in R_{out} nearly equal to R_{side} . Accordingly, we calcu-

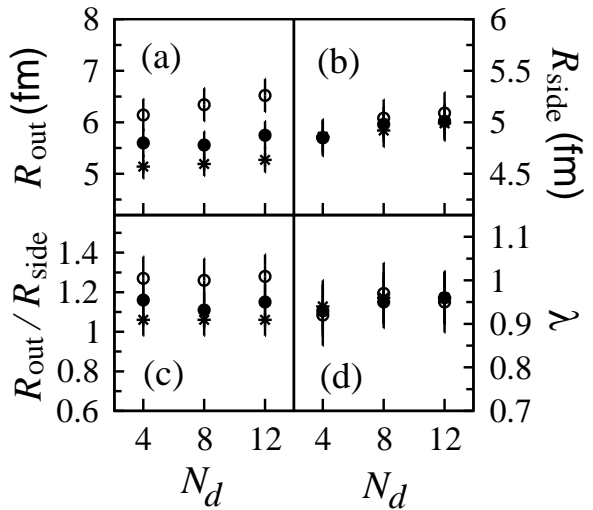


FIG. 3: Two-pion HBT results for the granular source of the droplets. The symbols \circ , \bullet , and \star are for the initial droplet radius $r_d = 2.0$, 1.5 , and 1.0 fm, respectively.

late next the two-pion correlation function for a Gaussian distribution source of N_d droplets. The spatial center-of-mass coordinates \mathbf{X}_d of the droplets are assumed to obey a static Gaussian distribution $\sim \exp(-\mathbf{X}_d^2/2R_G^2)$ [19, 20, 21]. Figure 3(a), 3(b), 3(c), and 3(d) give the HBT R_{out} , R_{side} , $R_{\text{out}}/R_{\text{side}}$, and λ as a function of the number of droplets N_d for different values of r_d . In this calculation, we take $T_f = 0.65T_c$ and $R_G = 5.0$ fm. The symbols \circ , \bullet , and \star correspond to $r_d = 2.0$ fm, $r_d = 1.5$ fm, and $r_d = 1.0$ fm, respectively. It can be seen that the radii R_{out} and R_{side} have a slowly increasing tendency as N_d increases but their ratio $R_{\text{out}}/R_{\text{side}}$ is almost independent of N_d . R_{out} decreases as r_d decreases but R_{side} is relatively independent of r_d . Consequently, the ratio $R_{\text{out}}/R_{\text{side}}$ decreases when r_d decreases. The ratio $R_{\text{out}}/R_{\text{side}}$ for $r_d = 1.5$ fm is about 1.15 which is much smaller than the result of about 3 for the single droplet source.

Finally, to study the effect of additional collective expansion of the droplets, we calculate the two-pion correlation function for an expanding source. The initial distribution of the droplets is the same Gaussian distribution as the above granular source, but the droplets are assumed to expand collectively with a constant radial velocity v_d after the initial time, in addition to their hydrodynamical expansion. Figure 4(a), 4(b), 4(c), and 4(d) give the HBT R_{out} , R_{side} , $R_{\text{out}}/R_{\text{side}}$, and λ for different values of v_d . In this calculation, we take the initial radius of the droplets to be $r_d = 1.5$ fm, the other parameters are the same as the above calculations for a static granular source. The symbols \circ , \bullet , and \star correspond to $v_d = 0, 0.3$, and 0.6 , respectively. The results in Figs. 4(a) and 4(b) show that R_{side} increases more rapidly with the droplet collective expansion velocity v_d than R_{out} . A radial expansion will increase the transverse size of the granular source and R_{side} . On the other hand, R_{out} mea-

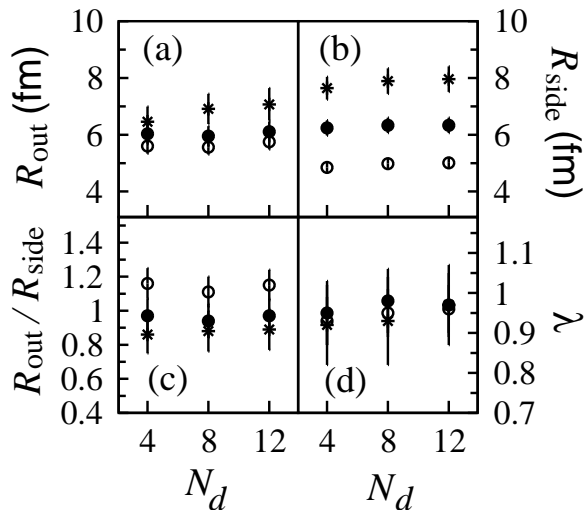


FIG. 4: Two-pion HBT results for the granular source with a radial collective expansion of the droplets. The symbols \circ , \bullet , and \star are for the expansion velocity $v_d = 0, 0.3$, and 0.6 , respectively.

sure the source life time and the spatial extension where the two pions are emitted with nearly parallel and equal momenta, and the additional radial boost modifies only slightly the spatial separation of these points for most cases. As a result, R_{out} does not increase as rapidly as R_{side} and $R_{\text{out}}/R_{\text{side}}$ is smaller at large v_d than at zero v_d (see Fig 1(c)). The ratio $R_{\text{side}}/R_{\text{out}}$ is of order 1 which is close to the observed value [1, 2].

In summary, we propose a simple model of granular source of quark-gluon plasma droplets to examine the HBT interferometry data. The droplets evolve hydrodynamically and pions are emitted thermally from the droplets at the freeze-out configuration characterized by a freeze-out temperature T_f . As the average freeze-out

time is proportional to the radius of the droplet, smaller droplet size allows pions to be emitted within a shorter time and the life-time of the source decreases, leading to a smaller HBT radius R_{out} . On the other hand, the HBT radius R_{side} depends on the width of the spatial distribution of the droplets and is insensitive to the initial size of the droplets. The ratio of R_{out} to R_{side} decreases significantly if the emitted source is granular in nature. Furthermore, R_{side} increases with the collective-expansion velocity of the droplets more rapidly than R_{out} . The ratio $R_{\text{out}}/R_{\text{side}}$ is about 1.15–0.88 for the collective-expansion velocity of the droplets from zero to 0.6, for the granular source with a Gaussian initial radius 5 fm and a droplet initial radius 1.5 fm. This $R_{\text{out}}/R_{\text{side}}$ ratio is close to the experimental values [1, 2]. The granular model of quark-gluon plasma may provide a possible explanation to the RHIC HBT puzzle. It may also lead to a new insight into the dynamics of the quark-gluon plasma phase transition as the formation of a granular structure is expected to occur in a first-order QCD phase transition [22, 23, 24, 25, 26, 27].

In order to bring out the most important features, we have neglected the multiple scattering effects on HBT interferometry [31, 40, 41], and have not considered how the granular nature of the plasma may arise from detailed phase transition dynamics [22, 26, 27]. The sizes of the droplets in a collision can also have a distribution. Future refinements of the present model to take into account these effects on $R_{\text{out}}/R_{\text{side}}$ will be of great interest.

WNZ would like to thank Drs. T. Barnes, V. Cianciolo, and G. Young for their kind hospitality at Oak Ridge National Laboratory. This research was supported by the National Natural Science Foundation of China under Contract No.10275015 and by the Division of Nuclear Physics, US DOE, under Contract No. DE-AC05-00OR22725 managed by UT-Battle, LC.

-
- [1] PHENIX Collaboration, K. Adcox et al., Phys. Rev. Lett. **88**, 192302 (2002).
[2] STAR Collaboration, C. Adler et al., Phys. Rev. Lett. **87**, 082301 (2001).
[3] D. H. Rischke and M. Gyulassy, Nucl. Phys. A **608**, 479 (1996).
[4] D. Teaney and E. Shuryak, Phys. Rev. Lett., **83**, 4951 (1999).
[5] U. A. Wiedemann and U. Heinz, Phys. Rept. **319**, 145 (1999).
[6] S. Soff, S. A. Bass, and A. Dumitru, Phys. Rev. Lett. **86**, 3981 (2001).
[7] R. M. Weiner, Phys. Rept. **327**, 249 (2002).
[8] S. Pratt, Nucl. Phys. A **715**, 389c (2003).
[9] S. Soff, S. A. Bass, D. H. Hardtke, and S. Y. Panitkin, J. Phys. G **28**, 1885 (2002).
[10] D. Molnár and M. Gyulassy, in Proceedings of Budapest '02 Workshop on Quark Hadron Dynamics, published in Heavy Ion Phys. **18**, 69 (2003), nucl-th/0204062.
[11] S. Soff, S. A. Bass, D. H. Hardtke, and S. Y. Panitkin, Phys. Rev. Lett. **88**, 072301 (2002).
[12] U. Heinz and P. Kolb, Nucl. Phys. A **702**, 269 (2002).
[13] Zi-wei Lin, C. M. Ko, and S. Pal, Phys. Rev. Lett. **89**, 152301 (2002).
[14] D. Teaney, Nucl. Phys. A **715**, 817 (2003).
[15] T. Csörgö and J. Zimányi, Acta Phys. Hung. New Series, Heavy-Ion Physics, **17**, 281 (2003), nucl-th/0206051.
[16] D. Molnár and M. Gyulassy, Phys. Rev. Lett. **92**, 052301 (2004).
[17] D. Seibert, Phys. Rev. Lett. **63**, 136 (1989).
[18] T. Kajino, Phys. Rev. Lett. **66**, 125 (1991).
[19] S. Pratt, P. J. Siemens, and A. P. Vischer, Phys. Rev. Lett. **68**, 1109 (1992).
[20] W. N. Zhang, Y. M. Liu, L. Huo, Y. Z. Jiang, D. Keane, and S. Y. Fung, Phys. Rev. C **51**, 992 (1995).
[21] W. N. Zhang, G. X. Tang, X. J. Chen, L. Huo, Y. M. Liu, and S. Zhang, Phys. Rev. C **62**, 044903 (2000).
[22] E. Witten, Phys. Rev. D **30**, 272 (1984).

- [23] L. P. Csernai and J. I. Kapusta, Phys. Rev. D **46**, 1379 (1992); L. P. Csernai and J. I. Kapusta, Phys. Rev. Lett. **69**, 737 (1992).
- [24] R. Venugopalan and A. P. Vischer, Phys. Rev. E **49**, 5849 (1994).
- [25] S. Alamoudi *et al.*, Phys. Rev. D **60**, 125003 (1999).
- [26] L. P. Csernai, J. I. Kapusta, and E. Osnes, Phys. Rev. D **67**, 045003 (2003).
- [27] J. Randrup, Phys. Rev. Lett. **92**, 122301 (2004).
- [28] D. H. Rischke, nucl-th/9809044.
- [29] E. Laermann, Nucl. Phys. A **610**, 1 (1996).
- [30] J. B. Blaizot and J. Y. Ollitrault, Phys. Rev. D **36**, 916 (1987).
- [31] W. N. Zhang, M. J. Efaaf, C. Y. Wong, and M. Khalilur, Chin. Phys. Lett. **21**, 1918 (2004); nucl-th/0404047.
- [32] L. D. Landau and E. M. Lifshitz, *Fluid Mechanics*, (Pergamon, New York, 1959).
- [33] P. Kolb and U. Heinz, nucl-th/0305084.
- [34] V. Schneider *et al.*, J. Comput. Phys. **105**, 92 (1993).
- [35] A. Harten, P. D. Lax, and B. van Leer, SIAM Rev. **25**, 35 (1983); B. Einfeldt, SIAM J. Numer. Anal. **25**, 294 (1988).
- [36] G. A. Sod, J. Fluid Mech. **83**, 785 (1977).
- [37] Chapter 17 of C. Y. Wong, *Introduction to High-Energy Heavy-Ion Collisions*, World Scientific, 1994.
- [38] S. Pratt, Phys. Rev. Lett. **53**, 1219 (1984); S. Pratt, Phys. Rev. D **33**, 72 (1986); S. Pratt, T. Csörgo, and J. Zimányi, Phys. Rev. C **42**, 2646 (1990).
- [39] G. Bertsch, M. Gong, and M. Tohyama, Phys. Rev. C **37**, 1896 (1988); G. Bertsch, Nucl. Phys. A **498**, 173c (1989).
- [40] C. Y. Wong, J. Phys. G **29**, 2151 (2003).
- [41] C. Y. Wong, in Proceedings of Quark Matter 2004, J. Phys. G **30**, S1053 (2004); hep-th/0403025.